First results from a 1.1-m-diameter superconducting monopole detector

J. Incandela, H. Frisch, and S. Somalwar
Department of Physics and The Enrico Fermi Institute, The University of Chicago, 5640 South Ellis Avenue, Chicago, Illinois 60637

M. Kuchnir
Fermi National Accelerator Laboratory, Batavia, Illinois 60510

H. R. Gustafson
The University of Michigan, Ann Arbor, Michigan 48109
(Received 26 December 1985; revised manuscript received 14 July 1986)

We present the design and performance of a superconducting induction magnetic-monopole detector with 1.1-m-diameter gradiometer loops. The detector demonstrates that gradiometers can be overlapped with no mutual inductance to yield high redundancy without increasing shield volume. One of two detector units was sensitive to the passage of monopoles through two overlapped gradiometers with 98% coincidence efficiency for 161 hours. The unit has a coincident sensitive area averaged over 4π sr of 4400 cm^2. No candidate events were observed, setting an upper limit on the flux of cosmic-ray magnetic monopoles of $f \lesssim 7.1\times10^{-11}$ cm^{-2} sr^{-1} sec^{-1} (90% C.L.). The detector was operated in ambient magnetic fields of $\sim$5—125 mG.

INTRODUCTION

It was first pointed out by 't Hooft[1] and Polyakov[2] that monopolelike states *are required* by grand unified theories which have a U(1) group, such as electromagnetism, imbedded in them. However, models of the early Universe have oscillated in their predictions of how many monopoles were created in the initial moments after the big bang: several years ago there were far too many, and now the prevailing prejudice is that there are far too few to be detectable. Unfortunately, the theoretical predictions for the number created depend on such factors as the mass of the monopole and the temperature of the reheating of the Universe, both of which are unknown.[3]

The status of experimental limits on monopole abundance has changed rapidly in the last few years.[4] The most stringent limits come from astrophysical observations, but many of these require that monopoles catalyze proton decay.[5] The Parker bound,[6] which is based upon the persistence of magnetic fields in the Galaxy, sets an upper limit on the flux of the order of 10^{-15} cm^{-2}sr^{-1}sec^{-1}, but also depends on the monopole mass. Big ionization detectors, such as those of Shepko and Webb in Texas,[7] and in the Baksan mine of the USSR,[8] set limits in the 10^{-14}-cm^{-2} sr^{-1}sec^{-1} range, but depend on how a monopole ionizes matter. A very clever experiment by Price, Guo, Ahlen, and Fleischer[9] looks for tracks left in ancient mica by monopoles which have picked up Al nuclei, but there are ways in which the monopoles could not pick up Al nuclei, and so would not leave a track. Finally, Faraday-induction detectors, which are open to direct calibration and depend upon well-understood, long-range effects of electromagnetism for their principle of operation, have been limited in the past to small areas by the requirements of low-field operation and the fact that loops had to be made much smaller than their magnetic shields to avoid inductive coupling. Large-area induction detectors would be very attractive if they could be built.

The technique of detecting magnetic monopoles by an induced current was suggested by Alvarez[10] and independently by Tassie.[11] Early experimental pioneers were Eberhard, Ross, Alvarez, and Watt[12] and Vant-Hull.[13] Recently the technique has gained wide publicity as a result of the Stanford experiment done by Cabrera.[14]

Induction detectors have grown in size by an order of magnitude per year for the past three years. Several groups including our own have shown that gradiometer loop configurations reduce inductive coupling to the superconducting shield, which allows larger area loops to be designed.[15]

In a previous experiment[16] our group has also shown that it is possible to operate induction detectors in ambient magnetic fields as high as $\sim$1—10 mG by using completely closed superconducting shields and isolating the detector from vibration. In that experiment each of two 0.6-m-diameter gradiometers was enclosed in an independent superconducting shield. The two shielded gradiometers were positioned to obtain some degree of coincident acceptance area. The width of the shields made it impossible to bring the gradiometer planes any closer together than $\sim$22 cm and consequently the coincident area was only one-half of the total available surface area of an individual gradiometer. In 151 d of live-time exposure there were no unexplained coincident signals of any size and no monopole signals observed individually in either detector loop. This enabled us to set a limit on the magnetic monopole flux at $f \lesssim 6.7\times10^{-12}$ cm^{-2}sr^{-1}sec^{-1} (90% C.L.) (Ref. 16). We may also extract from the data a limit on the rate of spurious monopole signals for each detector loop (Ref. 17) $\nu_s \lesssim 1.8\times10^{-7}$sec^{-1} (90% C.L.). The corresponding rate of accidental coincidence of spurious monopole signals is thus limited to $\nu_c \lesssim 10^{-13}$sec^{-1} for a sampling rate of 1 Hz. This corresponds to less than

one such event every 300 000 yr.

In view of the fact that single, unexplained monopole-like signals have been observed in ~ 1 yr exposure times of several induction detectors,[14,18] it is important to develop detectors with a high percentage of coincident detection area. This was first achieved for a small area with the Stanford three-loop detector.[19] Later, a group at IBM devised a scheme for obtaining nearly 100% coincidence in which planar gradiometers are used to construct a completely closed surface in three dimensions.[20] Except for the case in which a monopole passes through the superconducting filament of one of the gradiometers, this configuration will yield two signals in coincidence for a monopole passing through the detector volume. Several large-area detectors now under construction employ this technique.[21,22]

In this paper we present the first results from an induction detector which employs a new technique for obtaining a high percentage of coincident detection area. In this scheme symmetry considerations are used to design gradiometers with patterns that allow them to be directly overlapped with negligible inductive coupling. We call these "close-packed orthogonal gradiometers." For the experiment described in this paper the detector consists of two closed superconducting shields each containing two 1.1-m-diameter gradiometers. The two gradiometers in each unit are separated by only 1 cm to obtain $\sim 98\%$ coincidence efficiency. Data presented below indicate that the overlapped grids have less than 1% mutual inductive coupling.

The detector was cooled in an ambient magnetic field of $\sim 5-125$ mG which represents an order of magnitude increase over the field strength at cool down of our previous experiment.[16] As a result of the higher ambient fields, a higher density of trapped flux in the superconducting shields is expected. In spite of this condition the data presented here contain no unexplained coincident signals of any size[23] in a live-time exposure of 161 h. Although the exposure time is fairly short, the data would seem to indicate that the overlapped gradiometers do not couple to trapped flux in their common shields in such a way that changes in the configuration of the trapped flux bundles will induce currents simultaneously in both coils.[24] In this paper we will also discuss ways in which we believe close-packed orthogonal gradiometers can be used to obtain extremely reliable high coincidence induction detectors with areas as large as 100 m^2 sr to 1000 m^2 sr even when operated in relatively high ambient magnetic fields.

This experiment also includes several other special factors. First of all the new gradiometers apply the techniques of "distributed-parallel" and "series-parallel" layouts.[25] This allows them to be manufactured on a single side of plated circuit-board with minimal loss in coupling to the SQUID (Ref. 26). The gradiometer pattern itself is also different from before.[27] It is comprised of concentric circles with polarity alternation along the radius (see Fig. 1). By limiting polarity changes to one coordinate direction, a larger signal is obtained. The radial cell widths are chosen to give a uniform signal for monopoles penetrating a detector unit along all possible trajectories.

In Sec. I of this paper we present the design of the detector shield and gradiometers. In Sec. II the physical apparatus is described in some detail. Section III discusses the performance of the apparatus in two test runs. Finally, in Sec. IV we present our results and conclusions.

I. DETECTOR DESIGN

A. Shields

The detector loops are enclosed completely in superconducting Pb shields. The shields are cylindrical with a diameter of 112 cm. The end caps are spherically domed with a 4-m radius of curvature. The height of the shield cylinder varies from 17 cm at the cylinder walls to 24 cm along the axis. The Pb shields were formed by cold-spinning (Ref. 28) 1.0-mm-thick Pb sheets on a wooden form. The preformed Pb was then bonded to high-conductivity Cu which was also cold spun to mate smoothly to the Pb. The two metals were bonded with low-melting-point Ostalloy[29] metal which superconducts at about the same temperatures as Pb.

B. Gradiometer design

The inductive coupling of the gradiometers to the Pb shield is found by first calculating the field resulting from quantized vortex currents induced in the shield by a passing monopole.[30] For a monopole passing through a closed cylindrical volume with the trajectory and shield geometry[31] shown in Fig. 2, the remnant field in the shield is obtained from the scalar potential:[32]

$$\Phi(\rho,\phi,z)=-\frac{g}{R^2}\left[z+\sum_{m=0}^{\infty}\sum_{n=1}^{\infty}(1-\delta_{m0}\delta_{n1})J_m(k_{mn}\rho)\{J_m(k_{mn}\rho_1)\cos[m(\phi-\phi_1)]\cosh[k_{mn}(z-z_2)]\right.$$
$$\left.-J_m(k_{mn}\rho_2)\cos[m(\phi-\phi_2)]\cosh[k_{mn}(z-z_1)]\}\right.$$
$$\left.\times\{k_{mn}(1-m^2/\xi_{mn}^2)[J_m(\xi_{mn})]^2\sinh[k_{mn}(z_1-z_2)]\}^{-1}\right],$$

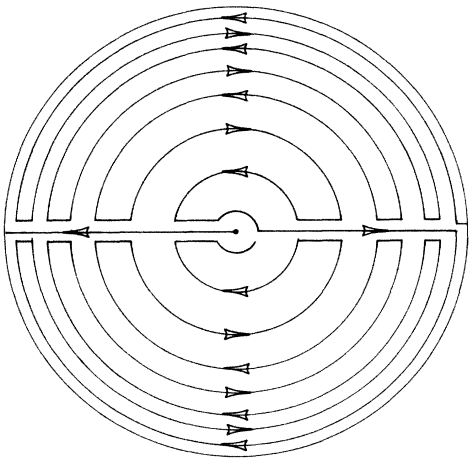

FIG. 1. Schematic diagram of the concentric circle gradiometer used in this experiment. Arrows indicate direction of current flow.

where

g = monopole charge ,

J_m = mth-order Bessel function ,

$k_{mn} = \xi_{mn}/R$,

ξ_{mn} = nth *root of* $dJ_m(x)/dx = 0$.

The factor $(1-\delta_{n1}\delta_{m0})$ is used to avoid the $m=0$, $n=1$ term which is a constant and does not contribute to the field.

The net flux impinging upon the gradiometer from the vortex currents in the shield is found by integrating the z component of the field, multiplied by the cell polarity (± 1), over the plane of the loops. For the trajectory shown in Fig. 2, the z component of field in the plane of the gradiometer is greatest in the vicinity of (ρ_1,ϕ_1) and (ρ_2,ϕ_2). Decoupling from the shield thus depends upon the cell widths in these regions. Calculations were done to determine the necessary cell widths to give better than 90% decoupling at all radii. These are plotted in Fig. 3 for various values of the ratio of diameter ($2R$) to height (H) of the cylinder. The plot indicates that the cells should diminish linearly in width near the cylinder wall. For a detector with $2R/H = 5$, this is most easily accomplished by the concentric loop pattern shown in Fig. 1. The response function of this system was calculated by generating many events randomly under the assumption of a uniform, isotropic flux of monopoles. The detector response is calculated for each event and a histogram of event probability versus signal size is obtained (see Fig. 4). The response function indicates better than 90% decoupling from the shield for 97% of all monopole trajectories. The low inductance of the concentric loop gradiometer also results in a signal more than twice the size of that from a square cell gradiometer with the same decoupling from the shield.

C. Close-packed orthogonal gradiometers

Consider a gradiometer composed of two identical cells of opposite polarity lying side by side in the xy plane. Such a pattern is odd in cell polarities for a reflection about the common borderline of the two cells. Consequently, any gradiometer which is even in cell polarities for this transformation, such as a simple rectangular loop as shown in Fig. 5, can overlap the two-cell gradiometer with no mutual inductive coupling. To see this, note that if we choose the y axis to be the reflection axis then the

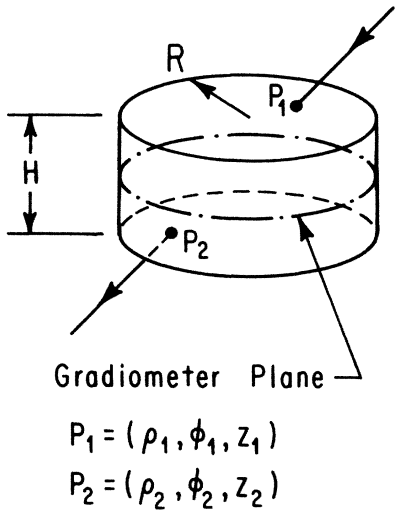

FIG. 2. Shield geometry and monopole trajectory used in calculating the field in the shielded volume. The field is produced by quantized vortex currents induced by the passing monopole at the points where the trajectory intersects the shield.

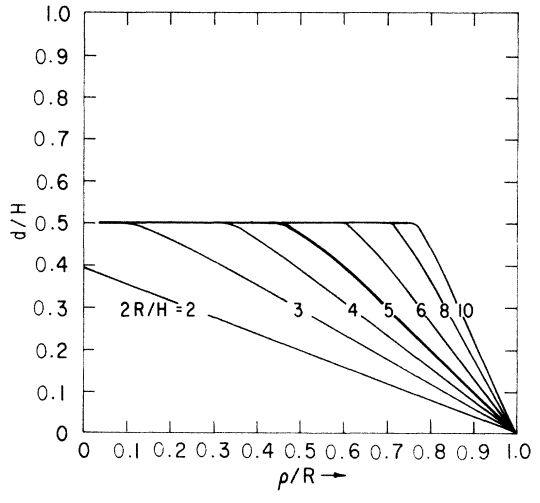

FIG. 3. Cell width vs radial position for $\gtrsim 90\%$ decoupling from the shield. Cell width is given in units of cylinder height H, and radial position is in units of the cylinder radius R. Different curves correspond to shields with different ratios of diameter to height as indicated. The shields in this experiment have a ratio of 5.

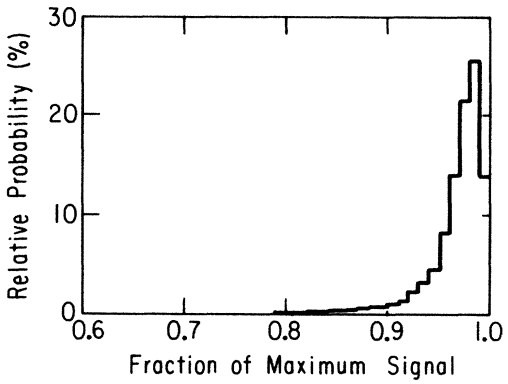

FIG. 4. The detector response curve. Inductive coupling of the gradiometer to the shield reduces the signal by an amount which depends upon the trajectory of the monopole. The curve indicates the probability of a passing monopole producing a particular signal size. The maximum signal corresponds to no inductive coupling. The probability for a signal to occur below 79% of maximum is zero.

field produced by a steady current in the two-cell gradiometer will have a component normal to the plane at an arbitrary point (x,y) which is exactly opposite to that produced at the point $(-x,y)$. Since the polarity of the overlapping loop is the same at both points, the flux in an infinitesimal area at (x,y) will cancel that at $(-x,y)$. Since (x,y) is chosen arbitrarily it follows that the net flux impinging upon the overlapping loop must integrate to zero.

Using symmetry arguments of this kind, orthogonal gradiometers can be found without explicit calculation of the fields produced by currents in the gradiometers. In particular, the argument given above can be generalized to state that any two gradiometers will be orthogonal (i.e., have no inductive coupling when directly overlapped) if there exists a symmetry transformation, leaving the shape and size of the gradiometers unchanged, for which one gradiometer is even in cell polarities and the other is odd.[32] By considering the group of such transformations

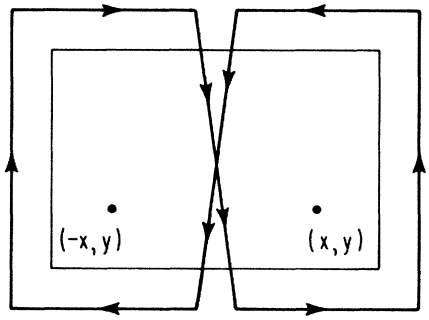

FIG. 5. A rectangular loop overlapping a two-cell rectangular gradiometer. The gradiometer can be made by twisting a rectangular loop about the center. A current induced in the gradiometer, flowing in the direction indicated by the arrows, would not induced a current in the overlapping loop. This is because the field at an arbitrary point (x,y) is exactly opposite to the field at the symmetric point $(-x,y)$. The net flux impinging upon the loop can thus be seen to integrate to zero.

associated with a particular gradiometer shape, gradiometer patterns can be classified according to their even and odd character under these transformations. For certain shapes it is then found that many patterns can be obtained which are all *mutually* orthogonal.

If, for instance, the common shape of the gradiometers to be overlapped has n-fold symmetry (i.e., n-distinct reflection axes and an n-fold rotation axis) then a study of the associated group of symmetry transformations reveals that a number $N=2(l+1)$ of mutually orthogonal patterns can be obtained from symmetry considerations alone, where l is the multiplicity of the factor 2 in a prime factorization of n (Ref. 33). For a square gradiometer, $n=4=2^2$ and so $l=2$ and $N=6$. A set of 6 mutually orthogonal square gradiometers is shown in Fig. 6 (Ref. 34). For circular shapes, the number of mutually orthogonal patterns which can be classified is virtually unlimited.[35]

We obtained orthogonality of the concentric loop gradiometers by designing the pattern to be antisymmetric in cell polarities upon reflection through a particular bisecting line (see Fig. 1). In this way, one gradiometer can be rotated 90° relative to the other so that any one cell in either gradiometer always symmetrically overlaps two cells of opposite polarities in the other gradiometer. Complete decoupling is demonstrated by an argument similar to

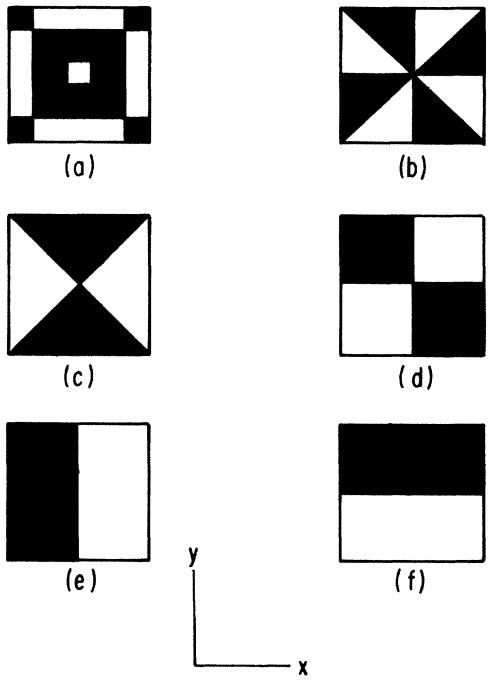

FIG. 6. A set of six mutually orthogonal gradiometers with square boundaries. Black and white regions have opposite polarity. Under at least one of the symmetry transformations of a square (an element of the group C_{4v}) each of the patterns (a)—(f) will be either even or odd with respect to cell polarities. Furthermore, for any two of the patterns, there is at least one transformation in C_{4v} for which one pattern will be even while the other will be odd so that gradiometers with these patterns can be expected to have no mutual inductive coupling.

that given above for the simple example of rectangular loops. In actuality, the gradiometers are separated by a 1-cm-thick G-10 support disc. The separation results in $\sim 2\%$ loss of coincident detection area. There is an additional 5% loss in coincident sensitive area resulting from the fact that no signal is generated if a monopole passes through the superconducting filament which is 0.254 cm wide.

II. PHYSICAL ATTRIBUTES OF THE APPARATUS

A. Overview (see Fig. 7)

The apparatus consists of two detector units suspended in vacuum and cooled by conduction. The shielded detector units are 1.12-m-diameter cylinders with spherically domed end caps. They are completed surrounded by thermal radiation and magnetic field shields. The radiation shields have diameters of 1.20 and 1.23 m and are maintained at nominal temperatures of 4.2 and 78 K, respectively.

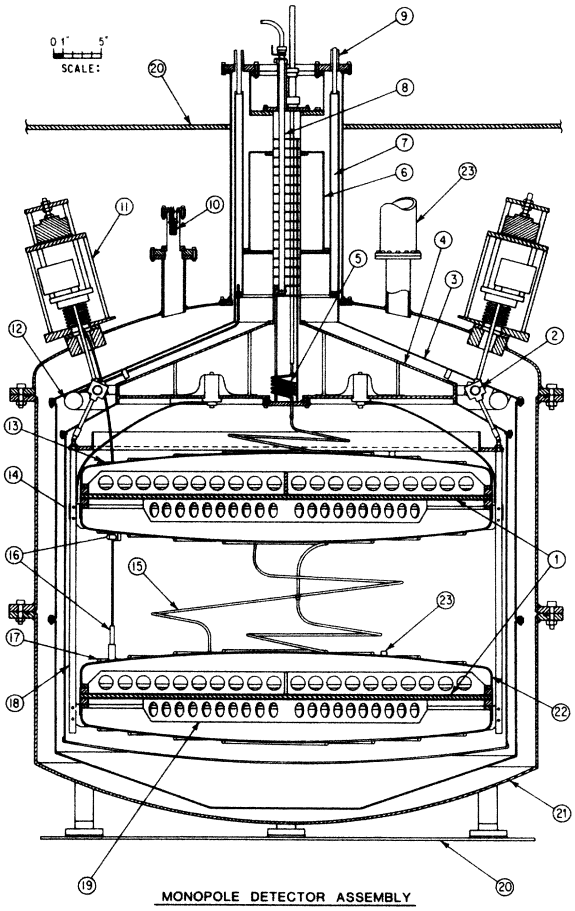

FIG. 7. The detector assembly: (1) gradiometer plane, (2) support ring, (3) 78 K radiation shield, (4) helium reservoir, (5) heat exchanger, (6) heat pick-up shroud, (7) nitrogen reservoir, (8) helium fill line, (9) nitrogen vent, (10) vacuum gauge, (11) vibration isolator, (12) nitrogen reservoir, (13) detector cooling coils, (14) 4 K radiation and magnetic field shield, (15) helium vent, (16) SQUID, (17) detector cooling coils, (18) copper support rods, (19) G-10 cross braces, (20) steel pipe, (21) vacuum vessel, (22) lead lined copper shield, (23) pseudopole feedthrough block, (24) vacuum port.

The vacuum vessel is made up of three pieces and has a total volume of 1800 l. A 70-l liquid-helium reservoir and a 30-l two-part liquid-nitrogen reservoir are also contained in the volume. The vessel is partially enclosed by an open steel pipe which is used for crude shielding from Earth's magnetic field.

B. Gradiometers and superconducting shields

The gradiometers are fabricated as conventional solder-plated circuit boards in which standard 60-40 solder is used as the superconducting filament. The plated circuit is inexpensive and simple to manufacture. The size of the gradiometers made it necessary to construct them by adjoining four circuit boards. Several solder joints were made between the boards to complete the circuit.

To inhibit vibration, the two gradiometers in each detector are strapped to opposite sides of a 1.0-cm-thick G-10 disk for rigid support. Additional stiffening is provided by G-10 cross braces captured by G-10 hoops at the perimeter of the assembly. The cross braces and support disc have patterns of holes cut in them to reduce their mass by 70%. This permits a more economical cool down. The gradiometers and support assembly are tightly fitted into cylindrical Pb shields with spherically domed end caps. The dome shape provides mechanical stability while a Cu shell enables rapid cooling to uniform temperatures.

C. Calibration solenoids ("pseudopoles")

Each detector unit has long slender solenoids piercing the shield and gradiometers. The solenoids can be excited with dc currents to core fluxes of either $3\phi_0$ or $30\phi_0$ ($\phi_0 = 2.07 \times 10^{-15}$ Wb), which induces currents in the shield and detector loops. These currents are indistinguishable from those that would be produced if a monopole with 1.5 or 15 units, respectively, of the expected Dirac charge were to penetrate the detector unit along the line occupied by the solenoid axis.[36] For this reason we have named these calibration devices "pseudopoles."

The top detector unit has eight pseudopoles used to calibrate the response of the detector for arbitrary monopole trajectories and to measure the inductive coupling of the overlapped gradiometers. The bottom detector unit has four pseudopoles. By comparing the response to these pseudopoles with those for similarly positioned pseudopoles in the top detector unit, the overall response of the bottom detector can also be determined.

D. SQUID's

The signals from the four gradiometers are continuously monitored by rf (radio-frequency) biased superconducting quantum interference devices[26] (SQUID's). The SQUID's are mounted directly onto the shielded detectors. The leads connecting the SQUID's to the rf heads

pass from vacuum to atmospheric pressure by means of vacuum feed-through connectors on vibrationally isolated suspension devices where the rf heads are attached. The superconducting leads from each gradiometer pass through the shield to their corresponding SQUID by means of a hole in a Pb block to which the squid is mounted. This completes the magnetic shielding of the superconducting detector circuit.

There are several important advantages to the SQUID mounting discussed above. Primarily, this scheme assures that the SQUID's, rf heads, and shielded gradiometers—which together comprise the principle components of the detector—are all part of the vibrationally isolated system. Thus, relative motions of the pieces are greatly reduced. Also, by placing the SQUID's in a vacuum, the vibration encountered in a bath of liquid helium is avoided. An equally important consideration is that by placing the SQUID's and signal leads inside of the closed aluminum vacuum vessel, the system is much less susceptible to rf interference. Finally, the placement of the SQUID's inside the 4.2 K radiation shield, which is solder coated to superconduct, provides additional shielding from low-frequency magnetic fields.

In order to use the SQUID's in this way, several modifications of the commercial design were necessary. In particular, 0.15-cm-diameter flexible stainless-steel tubing was used to shield the copper leads between the rf heads and the SQUID's. In two places this tubing was then replaced by 15-cm lengths of 0.30-cm-diameter copper tubing. The flexible tubing was necessary to enable the leads to follow the circuitous pathways between the rf heads and the SQUID's in the final assembly. The copper tubing segments are needed to cool the copper leads from 300 K at the rf heads to sufficiently low temperatures at the SQUID's so as to maintain the latter superconducting. The heat sinking of the leads was achieved by filling the tubes with low-vapor pressure grease[37] and connecting the copper sections to cold surfaces with high-conductivity copper straps. The length of the copper tubing sections was chosen to compensate for the low thermal conductivity of the grease.

E. Detector cooling

The total mass of the detector is ~ 230 kg. To cool this mass quickly and efficiently we hard-soldered a coil of 1-cm-diameter hollow copper tubing to the copper shells of the detector units. Helium gas can be circulated through the coil, passing first through a heat exchanger immersed in cryogenic fluid and then to the detector to absorb heat. The gas can then be vented to atmosphere or cycled again through the coil.

When the detector units have reached stable minimum temperatures, the cooling tubes are evacuated and sealed. The detector is maintained at these temperatures by conducting heat to the liquid-helium reservoir via flexible copper straps.

To operate economically at ~ 4.2 K the detector units must be shielded from 300-K thermal radiation. To this end they are completely surrounded by conducting surfaces maintained at 4.2 and 78 K. The shields are cooled by conduction to the liquid-helium and liquid-nitrogen reservoirs, respectively. To reduce the heat load on the cryogenic liquids the shields are wrapped in multiple layers of thermally insulated, highly reflecting aluminized Mylar.

F. Vibration isolation and environmental disturbance monitors

The detector units are suspended with copper rods attached to a *G*-10 ring. The ring is suspended by six hollow *G*-10 tubes from a stainless-steel ring. This load ring is in turn connected at three points to hollow *G*-10 rods which attach to flanges on the exterior of the vacuum vessel. The flanges are vibrationally isolated from the vacuum vessel by means of flexible bellows and critically damped inflatable cushions.[38]

In spite of the vibration isolation just described, some mechanical disturbances may still be transmitted to the detector or initiated by the relief of stresses in the detector units themselves. Such disturbances have been found to alter the detector signal and produce monopolelike dc offsets.[39] To discriminate such spurious signals from a real signal it is necessary to detect these infrequent disturbances.

In this experiment eight piezoelectric strain gauges[40] were used for this purpose. Four of the gauges were clamped to the SQUID lead tubes, two were placed on the copper shells of the detector units, and two were attached to the 4.2 K radiation shield. We found that the 115-kg detector units were the quietest objects in the apparatus. The SQUID lead tubes were therefore clamped to the units to reduce their vibration. In this configuration we found the SQUID signals were fairly insensitive to induced vibrations in the SQUID lead tubes (see Fig. 8). Magnetic field, rf radiation, and liquid-nitrogen fill-system pressure were also monitored as possible sources of spurious signals.

G. Reduction of ambient magnetic fields

The detector units and superconducting shields were cooled below the superconducting transition temperature in an average magnetic field of 35 mG which ranged from a minimum of 5 mG to a maximum of 125 mG. This is roughly ten times the field of our previous experiment.[16] To reduce the ambient field to this level, a 183-cm-diameter, 213-cm-tall steel cylinder was used. The cylinder was wrapped with vertical and horizontal coils of wire. We calculated an optimum current setting in the coils which minimizes the average field at the detector. This current setting was established during cool down. During the superconducting transition, a fraction of this field may be expelled from the detector region while the remainder is trapped at pin sites in the shields. The magnitude of the pinned field was not measured. The wide range of field values, and the consequent large average field, is due to the fact that we cannot zero out the field

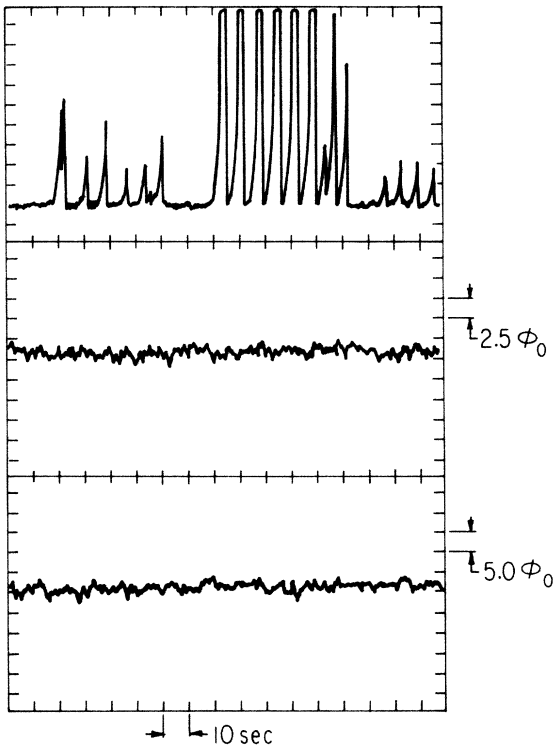

FIG. 8. Vibration sensitivity test data. The two SQUID signals for the bottom detector unit are shown below. The topmost channel is the summed signals of six strain gauges. Repeated tapping at various points on the apparatus, including the isolation mounts which suspend the detector units, is seen not to affect the signals.

over such large detector units given the size of our present steel shield.

H. Data acquisition

Data from the SQUID's and monitors were continuously recorded by an 8-channel chart recorder. Data could also be written to computer tape after being digitized by a 32-channel analog-to-digital converter (ADC). The results of this experiment are based on an analysis of the strip chart recordings.

III. TEST RUNS AND DETECTOR PERFORMANCE

A. Summary of two test runs

The detector was cooled down for a first time. All four SQUID's were found to be operating and the pseudopoles indicated an adequate signal size for a single Dirac-charge monopole. The inductive coupling of the close-packed gradiometers was also measured. Unfortunately, loose SQUID lead tubes caused the signals to be too strongly affected by vibration to allow a monopole flux measurement. The run was terminated to fix the vibration problem and to repair a vacuum leak.

A second cool down was begun at a later date. One SQUID for the top detector unit did not operate due to a change in heat sinking which caused it to warm above the superconducting temperature. In addition, a new vacuum leak developed leading to a high rate of liquid-helium consumption. However, we found that the vibrational sensitivity of the operating SQUID's had been dramatically reduced by clamping the lead tubes to the detectors. The bottom detector unit could therefore be used to detect monopoles unambiguously and was operated over a period of 12 days.

B. Decoupling of overlapped gradiometers and detector signal size

To measure the coupling of the overlapped gradiometers, two pseudopoles were positioned to penetrate a single cell in one gradiometer and two cells of opposite polarity in the other. By the symmetry of their placement, the stimulation of the pseudopoles leads to $6\phi_0$ (or $60\phi_0$ depending on the excitation current), of flux in one gradiometer and none in the other.[41] If the gradiometers are truly decoupled, the excited pseudopoles will then induce a current in only one gradiometer. Any coupling, on the other hand, would reduce this current while producing a corresponding nonzero current in the other gradiometer. From a series of repeated measurements (Fig. 9) of the signals induced in the gradiometers, the inductive coupling was determined to be less than 1%.

The signal sizes for trajectories at various radii were measured by exciting pseudopoles positioned at these radii. The induced signals were found to lie within a 5% range as expected. The maximum signal size for a single Dirac-charge monopole varied between 3.5 and 4.2 mV

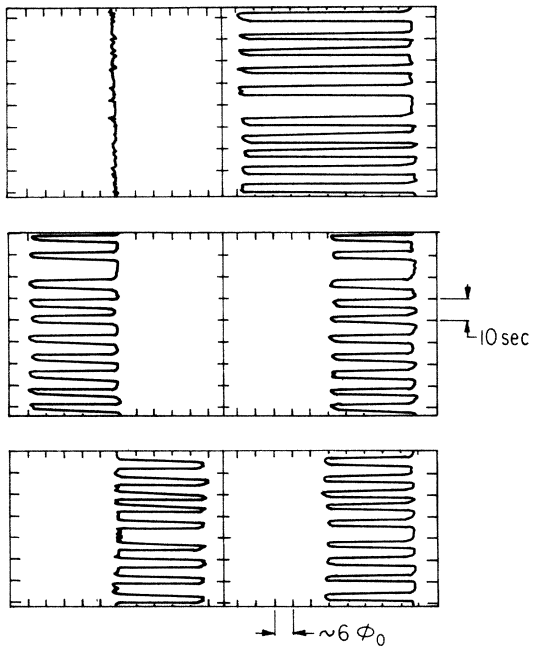

FIG. 9. Data from a test of gradiometer coupling. The $30\phi_0$ signal for each of two separate pseudopoles is measured simultaneously in each gradiometer. Both pseudopoles are then stimulated repeatedly. As expected, the steady-state signal is negligible in one gradiometer and doubled in the other.

(Ref. 42) for the four gradiometers as a result of variation in SQUID sensitivities. The dc offset of the SQUID signals was found to drift by less than ~ 1.2 mV/hr. With a low-pass filter of 1 Hz, an ac noise component of from 3—6 mV *pp* was also measured. At 0.1 Hz filtering the voltage signal-to-noise ratio[43] was between 6 and 10—1. The ac noise component is believed to be due to the large amount of trapped flux in the SQUID and/or because the SQUID's are being operated at temperatures too near to the critical temperature as a result of less than perfect heat sinking. Nevertheless, the dc offset corresponding to a monopole is clearly visible and unambiguous.

C. Sensitivity to environmental disturbances

Vibrational sensitivity was measured by tapping the apparatus at various places. Impulses could be imparted to the detector units and SQUID's by tapping the isolation devices to which the detector suspension rods and the SQUID lead tubes are attached. For tapping at all positions, the signals from the bottom detector unit were unaffected (see Fig. 8). Prior tests, completed before the SQUID tubes were clamped, induced signals as large as $\sim 50\phi_0$.

Sensitivity to external magnetic fields was measured by circulating 400 mA currents in the coils on the steel pipe surrounding the apparatus. The bottom detector unit signals varied by less than $2\phi_0$ for field changes of about 50 mG. The top detector unit signals indicated roughly 20 times this sensitivity. The detector units themselves are adequately shielded. We believe the remaining sensitivity to the external magnetic field is in the SQUID's themselves, which can easily be shielded. The reduced sensitivity of the bottom detector unit circuit was obtained by wrapping the SQUID's for this unit in 0.1-mm-thick Pb foil that extends roughly 10 cm along the SQUID lead tubes from the end of the niobium SQUID casing.

IV. RESULTS AND CONCLUSIONS

Chart recorder data from 12 days of operation of the bottom detector unit were scanned for monopolelike signal offsets. Live time corresponded only to those periods when no work was being done on the apparatus and no cryogenic fluids were being transferred. In addition, we demanded that both gradiometers be sensitive and that all monitors be operating. A live-time sample of 161 h was thus accumulated. No monopole candidates[44] were observed.

Single dc offsets observed in the two circuits which do not correlate with disturbance monitor signals are histogramed in Fig. 10. In one of the two circuits [Fig. 10(a)] the typical ac noise is ~ 5 mV *pp* and consequently offsets below ~ 3.0 mV cannot be counted at full efficiency.[45] Similarly the ac noise level in the other circuit is typically ~ 3.0 mV *pp* and so offsets below ~ 1.5 mV could not be included in the figure. There were no coincident offsets observed.

In the absence of coincident offsets we use the data for single offsets in the two gradiometers to estimate the rate of spurious monopole events due to accidental coincidence. In the noisier circuit there is one offset of ~ 3.7 mV which is consistent with the signal size expected for a monopole. From this one spurious signal in 161 h we obtain a spurious monopole rate[46] of $\nu_a \lesssim 6.6\times 10^{-6}$ sec^{-1} at the 90% C.L. for this circuit. The absence of such signals in the other circuit allows us to place a limit on the rate of false monopole events at $\nu_b \lesssim 3.9\times 10^{-6}$ sec^{-1} (90% C.L.), for this circuit. At a 1.0-Hz sampling rate it then follows that the rate of accidental coincidence of monopole size offsets is $\nu \lesssim 6.0\times 10^{-11}$ sec^{-1} (90% C.L.) or less than one every 500 yrs.

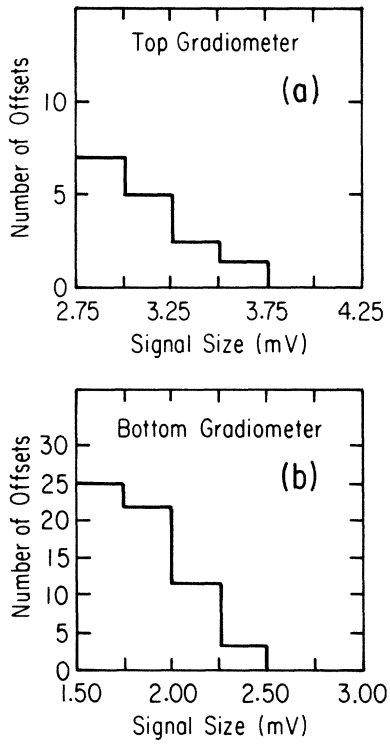

FIG. 10. Histograms of the dc offsets observed in each of the two overlapped gradiometer circuits during 161 hr of live time. Only those offsets which do not correlate with environmental disturbances are shown. In both cases the maximum monopole signal is expected to be ~ 4.2 mV. No coincident offsets were observed.

The total coincident area of the single operating detector unit, with two close-packed orthogonal gradiometers, averaged over all angles is 0.440 m^2. The exposure enables us to set a limit on the flux of cosmic-ray magnetic monopoles, $f \lesssim 7.1\times 10^{-11}$ cm^{-2} sr^{-1} sec^{-1} (90% C.L.). At this point the detector was warmed up to fix the vacuum leak. Although this flux limit is less stringent than the recent measurements of Incandela *et al.*,[16] Caplin, Hardiman, Koratzinos, and Schouten,[18] Berman *et al.*,[47] Cromar, Clark, and Fickett,[48] and Cabrera, Taber, Gardener and Borg,[49] each of which is in the 6×10^{-12} cm^{-2} sr^{-1} sec^{-1} region, the detector unit represents a larger detection area by a factor of 2.2, 2.8, 3.9, 4.7, and 9.4, respectively, over the detectors used in these previous experiments.[50]

If the detector units described in this paper were replicated to produce a 100—1000-m^2 sr array, the rate of ac-

cidental coincidence of monopole size offsets presented above would imply a rate of spurious coincident monopoles signals of 0.4—4.0 per year for the entire array, which is too large to allow a flux measurement at the Parker bound.[6] Based upon our experience in a previous experiment,[16] however, it is possible that the rate of spurious events may be reduced by as much as 2 orders of magnitude if the ambient magnetic field at cool down is reduced to $\sim 1-10$ mG.[51] Even without a reduction of the field the rate of spurious monopole signals can be drastically reduced by placing more than two closed-packed orthogonal gradiometers in the detector unit. For an accidental rate of monopole size offsets per gradiometer as high as $\nu \sim 6.6 \times 10^{-6}$ sec^{-1}, as presented above, the rate of accidental triple coincidence of monopole size offsets for 1.0-Hz sampling rate is $\nu_3 \sim 2.9 \times 10^{-16}$ sec^{-1} or one event every 100 000 000 yr. This translates into a spurious monopole signal rate, for a 1000-m^2 sr array, of one every 100 000 yr which is more than adequate to measure a monopole flux at the level of the Parker bound.

We conclude from the test runs of this apparatus that induction detectors with gradiometer loops in excess of 1-m diameter per SQUID can be constructed and operated in magnetic fields as high as 5—125 mG with a spurious monopole size signal rate $\nu \lesssim 6.6 \times 10^{-6}$ sec^{-1} (90% C.L.) per gradiometer. Furthermore, we have demonstrated that by means of close-packed orthogonal gradiometers, high redundancy of signal can be obtained without increasing detector volume. The detector units used in this experiment could be replicated as the subunits of a large planar array sensitive to a monopole flux at the Parker bound,[6] possibly by operating in a lower ambient field ($\sim 1-10$ mG), and certainly by adding a third gradiometer to the stack of close-packed orthogonal gradiometers to obtain near to 100% triple coincidence acceptance area.

ACKNOWLEDGMENTS

We thank J. Matthews, A. Green, A. Amiry, E. Weatherhead, R. Northrop, R. Gabriel, and L. Fiscelli of the University of Chicago for their excellent mechanical and design work, R. Smith of Fermilab for loan of a Dewar, H. Jostlein[52] of Fermilab for the loan of an ion gauge controller, and A. Guthke and C. Kendzione of Fermilab for loan of a turbo pump, and Zachary Incandela for help with our thermometry system. We also thank J. Tague and the crew of Lab 2 at Fermilab for allowing us to use their facilities for reconstruction and testing of the SQUID's. This research was supported by the National Science Foundation, the Department of Energy, and the University of Chicago Physical Sciences Division. This work was presented as a thesis chapter to the Department of Physics, The University of Chicago, in partial fulfillment of the requirements of the Ph.D. degree.

[1]G. 't Hooft, Nucl. Phys. **B79**, 276 (1974).

[2]A. M. Polyakov, Pis'ma Zh. Eksp. Teor. Fiz. **20**, 439 (1974) [JETP Lett. **20**, 194 (1974)].

[3]For a recent detailed review of theory and experiment, see *Monopole '83,* edited by J. Stone (Plenum, New York, 1983).

[4]See, for example, the reviews of H. Frisch, in *First Aspen Winter Conference,* 1985, edited by M. Bloch (Ann. N.Y. Acad. Sci. Vol. 461) (New York Academy of Sciences, New York, 1986); and S. Errede, in *ICOBAN 84,* proceedings of the International Colloquium on Baryon Nonconservation, Park City, Utah, 1984 (University of Wisconsin, Madison, 1984).

[5]See, for example, M. Turner in the proceedings of the *First Aspen Winter Conference,* Ref. 4; K. Freese, M. S. Turner, and D. N. Schramm, Phys. Rev. Lett. **51**, 1625 (1983).

[6]E. N. Parker, Astrophys. J. **163**, 225 (1971); M. S. Turner, E. N. Parker, and T. J. Bogdan, Phys. Rev. D **26**, (1982).

[7]M. J. Shepko and R. C. Webb, in *The Santa Fe Meeting,* proceedings of the 1984 Meeting of the Division of Particles and Fields of the American Physical Society, edited by T. Goldman and M. Nieto (World Scientific, Singapore, 1985).

[8]E. N. Alexeyev, M. M. Boliev, A. E. Chudakov, B. A. Makoev, S. P. Mikheyev, and Yu. V. Sten'Kin, Lett. Nuovo Cimento **35**, 413 (1982); also see E. N. Alexeyev, M. M. Boliev, A. E. Chudakov, and S. P. Mikheyev, in *Proceedings of the Nineteenth International Cosmic Ray Conference,* La Jolla, 1985, edited by F. C. Jones (Goddard Space Flight Center, Greenbelt, MD, 1985), p. 250.

[9]B. Price, S. L. Guo, S. P. Ahlen, and R. L. Fleischer, Phys. Rev. Lett. **52**, 1265 (1984).

[10]L. W. Alvarez, Lawrence Berkely Laboratory Report No. 470, 1963 (unpublished).

[11]L. J. Tassie, Nuovo Cimento **38**, 1935 (1965).

[12]P. H. Eberhard, R. N. Ross, L. W. Alvarez, and R. D. Watt, Phys. Rev. D **4**, 3260 (1971).

[13]L. L. Vant-Hull, Phys. Rev. **173**, 1412 (1968).

[14]B. Cabrera, Phys. Rev. Lett. **48**, 1378 (1982).

[15]H. Frisch as discussed by C. C. Tsuei, in *Magnetic Monopoles,* edited by R. A. Carrigan, Jr., and W. P. Trower (Plenum, New York, 1983), pp. 209—211; C. D. Tesche, C. C. Chi, C. C. Tsuei, and P. Choudhari, Appl. Phys. Lett. **43**, 384 (1983); J. G. Park and C. N. Guy, Blackett Laboratory report, 1982 (unpublished).

[16]J. Incandela, M. Campbell, H. Frisch, S. Somalwar, M. Kuchnir, and H. R. Gustafson, Phys. Rev. Lett. **53**, 2067 (1984).

[17]In the experiment of Ref. 16 being discussed here, there was $\sim 1\%$ probability that a monopole passing through a shielded gradiometer would produce a dc offset less than 3.2 mV. The remaining 99% probability corresponded to a signal in the range [3.2, 5.0] mV. The spurious signal rate presented here is based upon the absence of dc offsets in the high-probability region. It is calculated as the inverse of the exposure time multiplied by a factor of 2.3 obtained from the Poisson distribution for $n = 0$ to obtain a 90% C.L. limit.

[18]A. D. Caplin, M. Hardiman, M. Koratzinos, and J. C. Schouten, Nature (London) **321**, 402 (1986).

[19]B. Cabrera, R. Gardner, and R. King, Phys. Rev. D **31**, 2199 (1985).

[20]C. C. Tsuei, in *Magnetic Monopoles,* edited by Richard A. Carrigan, Jr. and W. Peter Trower (Plenum, New York, 1983), p. 214.

[21]Chi *et al.*, in *Monopole '83,* Ref. 3, p. 459.

[22]Cabrera *et al.*, in *Monopole '83,* Ref. 3, p. 446.

[23]In fact there was only one pair of coincident offsets observed which correlated with an environmental disturbance. The disturbance registered on three environmental monitors. In addition, both offsets were below the size expected for a single Dirac-charged monopole passing through the detector.

[24]The possibility that this would not be the case is one criticism of the overlapped gradiometers scheme which we have encountered. See Ref. 47.

[25]S. Somalwar, H. Frisch, J. Incandela, and M. Kuchnir, Nucl. Instrum. Methods **226,** 341 (1984).

[26]Superconducting Quantum Interference Device, manufactured by B.T.I. Corporation, 4174 Sorrento Valley Boulevard, San Diego, CA 92121.

[27]The concentric circle gradiometer discussed here with some cells diminishing linearly in width with increasing radius bares some similarity to a circular gradiometer discussed several years ago by the IBM group. [See C. C. Chi *et al.*, IBM Technical Disclosure Bulletin **26,** 11 (1984); **26,** 6036 (1984).] Both patterns correspond to attempts to minimize the self-inductance of the gradiometer while preserving null coupling to changing magnetic fields. The gradiometer discussed in this paper is based upon an attempt to limit cell polarity alternation to one coordinate direction only which is not true in the IBM approach. The single azimuthal polarity alternation (see Fig. 1) is included in our design to enable close packing of two gradiometers as discussed later in this paper. It is not necessary for decoupling from the magnetic field.

[28]Helander Spinning Co., 4108 West Division Street, Chicago, IL 60651.

[29]Ostalloy 158 (melts at 158 F) Arconium Corporation, 400 Harris Avenue, Providence, RI 02909.

[30]For alternative calculations in different geometries, see Refs. 19 and 15(c).

[31]The right circular cylinder with flat end caps is used to approximate our actual domed end-cap geometry by choosing z_1 and z_2 in Fig. 2 to correspond to the vertical positions at which the trajectory would intersect the domed end caps. By comparison with pseudopole signals, this approximation is determined to be good to $\pm 5\%$.

[32]For more details, see J. R. Incandela, Ph.D. thesis, the University of Chicago.

[33]The group C_{nv} of symmetry transformations of an object with n-fold symmetry is generated by two transformations, a rotation through an angle $2\pi/n$, denoted C_n, together with any one of the n reflections denoted by $m_n(i)$, $i=1,\ldots,n$. Once the even or odd character of a gradiometer pattern is fixed for the two generator transformations, then the even or odd character will be fixed for all of the transformations in C_{nv}. Since $m_n(i)^2=E$, the identity, it is possible to have patterns which are even or odd under m_n (i). If n is odd then patterns can only be even under C_n since otherwise C_n^n would be odd which is not possible since $C_n^n=E$. In this case we have only two possible mutually orthogonal patterns, corresponding to $(C_n,m_n(i))=(+,+)$, $(+,-)$ where the shorthand notation of a plus (minus) sign is used to represent an even (odd) character under the respective transformations in the ordered pair to the left of the equal sign. If n is even, then C_n can be odd and two more patterns can be added to the orthogonal set, i.e., $(C_n,m_n(i))=(-,+)$, $(-,-)$. Similarly if $n/2$ is even we may add two more patterns, namely, $(C_n^2,m_n(i))=(-,+)$, $(-,-)$, and so on. In this way it is seen that $N=2(l+1)$ patterns can be found where l is the multiplicity of the factor 2 in a prime factorization of n. (See Ref. 32.)

[34]Each pattern in Fig. 6 could be replaced by another pattern which has the same even/odd symmetry character under the transformations of the group C_{4v}. Patterns (a)—(d) have even or odd character for all of the transformations in C_{4v}. Patterns (e) and (f) are odd under the 180° rotation C_4^2 so that they have no symmetry character under C_4 or C_4^3. They are also even or odd with respect to reflections about the x and y axes and therefore they could be replaced by patterns which are odd under C_4^2 but even and odd for reflections about the diagonals $x=\pm y$. These latter patterns have only the transformations C_4^2 in common with patterns (e) and (f) and so will not be orthogonal to these patterns. (See Ref. 32.)

[35]In the case of a circle, the group of symmetries is infinite since the circle is symmetric for infinitesimal rotations about an axis through its center and perpendicular to the plane. For systems with continuous symmetries of this kind an infinite number of mutually orthogonal patterns can, in principle, be found. (See Ref. 32.)

[36]See H. Frisch as discussed by Tsuei, in *Magnetic Monopoles,* Ref. 15 or Incandela, in *Monopole '83* (Ref. 3), pp. 462 and 463.

[37]Apiezon N, Apiezon Products Ltd., 4 York Road, London S.E.1, England.

[38]Stabl-Levl Mount No. SLM-3, Barry Wright Corp., 700 Pleasant Street, Watertown, MA 02172.

[39]This effect has been observed by virtually all monopole hunters using SQUID systems. For a detailed study see, F. R. Fickett, M. Cromar, and A. F. Clark, in *Monopole '83* (Ref. 3), pp. 477—480.

[40]Model SG-2M, Gulton Industries, Inc., 212 Durham Avenue, Methuchen, NJ 08840. We thank M. Cromar for making us aware of these devices and for showing us how to use them.

[41]In the absence of a passing monopole there is, of course, no net flux change since a superconducting loop will obey Lenz's law exactly. Consequently, one gradiometer induces a current in response to the $6\phi_0$ or $60\phi_0$ pseudopole flux. In the other gradiometer, the net pseudopole flux is zero and no current is induced.

[42]In designing the gradiometer, an upper limit for the self-inductance was obtained by summing the separately calculated inductances of the circular loops in the pattern. This led us to a lower limit for the signal size of ~ 3.0 mV.

[43]The signal is dc and the dc noise was only 1.2 mV/hr, enabling us to obtain a much higher signal to noise ratio by appropriate signal processing.

[44]A monopole candidate would correspond to coincident signals in the high probability response region (0.8—1.0 of maximum signal, see Fig. 4) for overlapped gradiometers. The monitors must also indicate that no environmental disturbance is occurring at the time of the event.

[45]For offsets that are smaller than about one-half of the ac peak-to-peak noise it is difficult to determine the signal rise time in a visual scan of the chart recorder data for which the SQUID's were filtered at 1.0 Hz. For this reason fast and slow dc offsets cannot be easily distinguished. The exclusion of offsets below the levels mentioned does not alter our determination of spurious monopole signal rates discussed later.

[46]We calculate a rate at 90% C.L. using the Poisson distribution: to obtain this rate we divide 3.6 by the exposure time, where the number 3.6 is obtained from the Poisson distribution for $n=1$. This yields a larger estimate of the rate of offsets for this circuit than would be obtained by using the in-

verse of the exposure time alone.

[47]S. Bermon, P. Chaudhari, C. C. Chi, C. D. Tesche, and C. C. Tsuei, Phys. Rev. Lett. **55**, 1950 (1985).

[48]M. W. Cromar, A. F. Clark, and F. R. Fickett, Phys. Rev. Lett. **56**, 2561 (1986).

[49]B. Cabrera, M. Taber, R. Gardner, and J. Borg, Phys. Rev. Lett. **51**, 1933 (1983).

[50]With both detector units operating, the coincident area averaged over solid angle is 0.75 m^2. This would represent an increase in detection area of 3.6, 4.4, 6.4, 7.5, and 15, respectively, compared to the experiments listed.

[51]Of course the detector unit in our current experiment has a larger area ($\sim$4 times) and other features which are different from our previous detector so that the reduction in spurious signal rate cannot be guaranteed to occur upon cooling in lower ambient fields. It has been our experience however that this kind of reduction with reduced fields does take place (see Ref. 32).

[52]We regret that we inadvertently did not acknowledge H. Jostlein in our previous publication (see Ref. 16 above).